Proc. of SPIE Vol. 0181, Contemporary Optical Systems & Components Specifications, ed. Robert E. Fischer (Apr 1979) Copyright SPIE

Typical error budget for testing a high-performance aspheric telescope mirror

C. F. Robbert, P. R. Yoder, Jr. and L. A. Montagnino
Electro-Optical Division, Perkin-Elmer Corporation
Norwalk, Connecticut 06856

Abstract

In choosing the proper technique for testing the optical figure of a high-performance aspheric mirror, it is appropriate to prepare a complete error budget for the test and to analyze the individual elements thereof to ensure that the measurement uncertainty is within acceptable limits. Such an error budget has been defined for the Hindle Shell test of a convex hyperboloidal secondary mirror for a hypothetical high-performance Cassegrain telescope system. A residual figure error of $\lambda/80$ rms at $\lambda = 0.6328\ \mu m$ is assigned to this mirror. This paper establishes the rationale for the error budget and develops specifications for the test system and equipment components. The importance of measuring and subtracting the error contributions of the test set-up and of data processing to remove certain systematic errors is pointed out.

Introduction

The manufacturing requirements for a high-performance aspheric mirror extend beyond the mirror itself. The test configuration for proving the quality of the aspheric usually requires a number of high-quality components. We will examine these requirements for a convex hyperboloidal mirror by way of illustration. The test configuration errors are identified and an error budget established. This budget is used to show that in a null test, errors due to the surface and the fixed and random errors of the test setup cannot be separately identified. All the "errors" could be attributed to the mirror surface. It will be shown that the fixed errors of the test setup will be reduced to a small data reduction uncertainty by measuring the component contributions to the test setup wavefront and subtracting these in an appropriate manner from the total.

Our considerations start with an understanding of the geometry of the conicoid of interest since this allows us to select a test configuration which satisfies that particular geometry. Once the test configuration has been selected, the components of the test (interferometers, auxiliary optics, etc.) can be identified. These elements of the test instrumentation are then examined quantitatively for their contributions to the degradation of the test wavefront. This identifies a preliminary error budget. It is shown that tightening the tolerances on error contributions from the components of the test is of limited value.

The Aspheric

The sphere has only two geometric properties of major concern: its radius of curvature, and the quality of its spherical surface. In the case of a conic however, an extra property is imposed and the original two properties are usually more stringently controlled. This new property is the sagittal departure of the surface from the mathematical expression for some reference sphere.

The optical designer will choose an expression for the surface that relates its desired contour to the paraxial or vertex radius. This is meaningful since the vertex radius is used in calculating the conjugate relationships. The asphericity is then specified to control the spherical aberration.

On the other hand, the manufacturer will choose a different expression for the same surface. The reference sphere chosen will be that which best relates to the manufacturing process. This may be an edge radius, the best fit shpere, or some other reference sphere.

The metrologist's job is to measure and certify the parameters of the mirror. In review, these are: the reference radius, the aspheric contour (departure from the reference radius) and the quality of this aspheric surface. To verify these parameters we look to the reason for the original selection of the specific conicoid. Namely, for any given conicoid there are specific stigmatic points. If we construct our test around these stigmatic points we have a true null test. To illustrate this we will specifically examine a convex hyperboloidal mirror.

The Hyperboloid

Figure 1 shows the geometric properties of a hyperboloidal secondary mirror. In the Cassegrain telescope configuration, the primary would focus at F_1. The secondary would then reflect this converging cone to F_2. By making the secondary a hyperboloid, this relay func-

tion is accomplished without on-axis aberration.

The vertical line Y represents a plane of symmetry between the hyperboloid's two sheets from which the mathematical constants "a" and "c" are derived. F_1 and F_2 are conjugate foci. These positions are related to each other by the (positive) distances f_1 and f_2 in the classical thin lens equation:

$$\frac{1}{f_1} - \frac{1}{f_2} = \frac{2}{R_V}$$

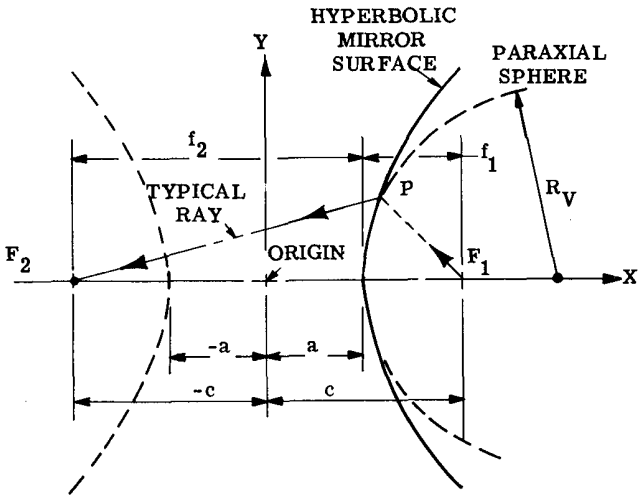

Fig. 1. Geometry of a hyperboloidal mirror.

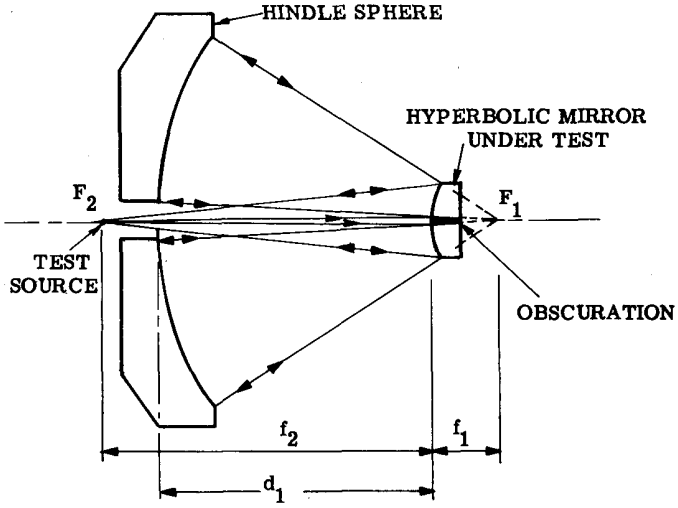

Fig. 2. Hindle sphere test configuration.

where R_V is the vertex radius of the hyperboloidal surface. The focal lengths of f_1 and f_2 are derived from the geometry.

$$f_1 = c - a$$

$$f_2 = c + a$$

The conicoid's eccentricity "e" is the ratio of c/a. This can be shown to be related to the focal lengths by

$$e = \frac{f_2 + f_1}{f_2 - f_1}$$

Note that the parameters R_V,e are controlled via their relationship to the two stigmatic points F_1 and F_2. Our test configuration should conform to these relationships if we want a null test.

Test Configuration

The Hindle Sphere test[1], shown in Figure 2, satisfies the basic requirements via an autostigmatic arrangement. The focus of a suitable interferometer is located at F_2, the farther focal point of the surface under test. The beam originates at F_2. After reflection from the hyperboloidal surface under test, the beam appears to come from the conjugate focus F_1. By placing the spherical reference surface of the Hindle sphere at a proper spacing, i.e., with its center of curvature at F_1, the test beam will auto-reflect to focus back at F_2. The interferometer will then evaluate the surface in a test configuration whose geometry is similar to the way the mirror will be used. The secondary surface is doubled-passed by the test beam which increases the sensitivity of the test by a factor of two.

The Hindle Sphere test has three key disadvantages for some applications:

(1) It introduces an obscuration

(2) It requires a large precision spacing

(3) It requires the fabrication of a large, high-quality reference surface.

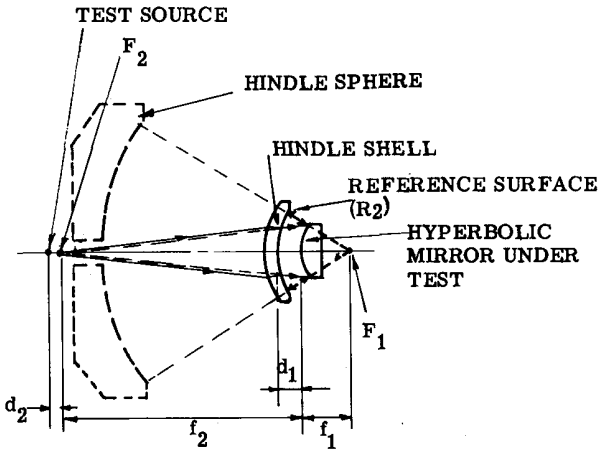

Fig. 3. Hindle shell test configuration.

These disadvantages are overcome by a variation of this test proposed by Simpson, et al[2] known as the Hindle Shell test. This is shown in Figure 3. The Hindle Shell test configuration allows one to test the secondary without obscuration, the size of the required Hindle Shell is typically just slightly larger than the part being tested, and the critical spacing is small. The Hindle Shell functions in exactly the same way as the Hindle Sphere except that the source is slightly displaced from F_2 due to refraction at the shell.

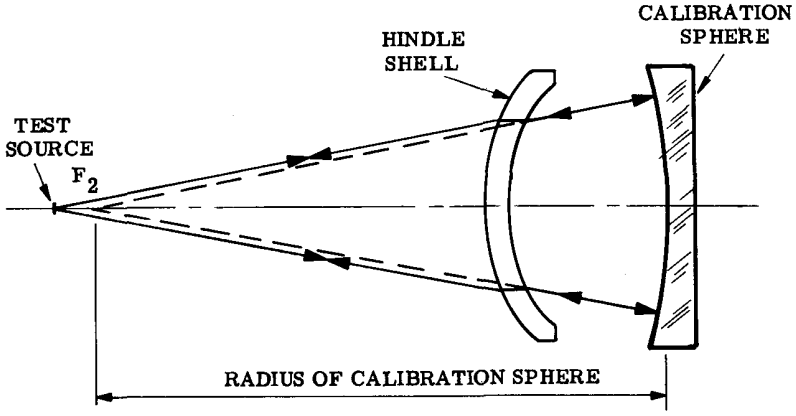

Fig. 4. Establishing the point F_2.

Let us assume that the vertex radius of the secondary has been measured by an independent technique. With this parameter fixed, the conjugate foci are the only axial degrees of freedom which need to be established. The point F_2 is fixed by utilizing a high quality calibration sphere as shown in Figure 4. The focus of the interferometer is placed at the center of curvature of the calibration sphere to within a small depth of focus. The accuracy of coincidence is limited primarily by interferogram data reduction. The Hindle Shell is now inserted.

The shell will introduce an axial shift of the interferometer focus since it has some power and thickness. This change in position should be within the adjustment range of the interferometer focus so precision is not lost by this step. The alignment of the Hindle Shell in tilt and transverse displacement is controlled by evaluating the interferogram for coma; proper alignment being indicated when coma is minimized.

Figure 5 shows how F_1 is established by locating the center of curvature of the reflective beamsplitter reference surface (R_2) of the Hindle Shell. Several techniques are available for this standard measurement. An autoreflecting microscope or an interferometer could be used. The latter will be chosen in our discussion for reasons which will become obvious.

The hyperboloid can now be inserted at the proper spacing from R_2 and F_1. This is generally critical so great care must be exercised here.

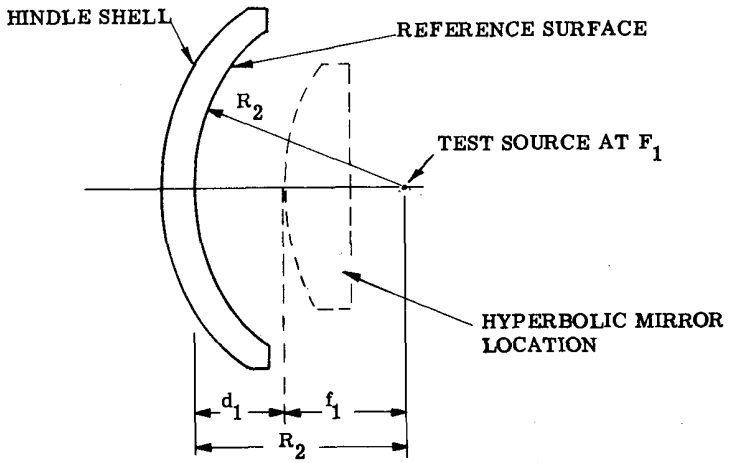

Fig. 5. Establishing the point F_1.

Error Sources

The test configuration is now established; but what are our sources of error and their magnitudes? Let us assume that we require the hyperboloid to have a figure which does not vary from the ideal contour by more than $\lambda/80$ rms at the test wavelength. Table 1 is a first cut at an error budget for the test.

Table 1. Test Configuration Wavefront Error Sources

Source of Error	Typical Double-Pass rms Contribution
1. Hindle Shell Test, Design Residual	λ /150
2. Hindle Shell Test, Opto-Mechanical Uncertainties	λ /200
3. Hindle Shell Test, Alignment Uncertainties	λ /500
4. Hindle Shell Reference Surface Figure Error (λ/80)	λ /40
5. Hindle Shell Transmitted Wavefront Error	λ /40
6. Interferometer Wavefront Error	λ /80
Subtotal, Instrumental Errors =	λ /26
7. Data Reduction Uncertainties	λ /200
8. Secondary Mirror Surface Error (λ/84)	λ /21
Total Measured Wavefront =	λ /16
Implied Secondary Surface Error = 1/4 Total =	λ /65

Let us now consider the listed sources of error in sequence.

Hindle Shell Test, Design Residual

The actual optical layout of the test needs to be evaluated. The Hindle Shell has axial thickness and power which will contribute aberration to the setup. The convex surface of the Hindle Shell can be designed to minimize this effect. For our example, we have arbitrarily chosen a reasonable single-pass contribution of $\lambda/300$ to the test wavefront. The wavefront interferogram will show λ/150 in double pass.

Hindle Shell Test, Opto-Mechanical Uncertainties

The radii of the Hindle Shell, thickness, and spacings of the test components will be measured to within some accuracy limits. The uncertainty in these measurements introduces an uncertainty in the design. This uncertainty is budgeted at $\lambda/200$ wavefront error.

Hindle Shell Test, Alignment Uncertainties

The alignment (tilt, and decenter) of the test components can be controlled by minimizing observed coma. By conducting a sensitivity analysis we could demonstrate that this would contribute only $\lambda/1000$ for a single-pass contribution or $\lambda/500$ error in the wavefront.

Hindle Shell Reference Surface Figure Error

This surface is seen once in the test so the wavefront error is twice its surface error. Thus, the assumed $\lambda/80$ surface contributes $\lambda/40$ to the test wavefront.

Hindle Shell Transmitted Wavefront Error

The surfaces R_1 and R_2 and the material inhomogeneity will distort the test wavefront. The inhomogeneity (Δn) would be on the order of $\pm 10^{-6}$ or greater. For a 5-cm thick shell at $\lambda = 0.6328$ μm, this corresponds to a single-pass OPD of $\lambda/12.7$. If this is not reduced, the total wavefront error would be dominated by this error. If the inhomogeneity is smoothly varying then one could monitor the transmitted wavefront and polish R_1 of the shell until the transmitted wavefront is more satisfactory. It should be noted that power and tilt can be removed directly. With these considerations we have budgeted $\lambda/80$ for a single-pass contribution.

Interferometer Wavefront Error

Any manufactured interferometer will have a wavefront which is not perfect. We have assumed it has a double-pass error of $\lambda/80$.

Data Reduction Uncertainties

Whenever an interferogram is interpreted there is a residual uncertainty which depends on many factors such as scanning limitations, curvature of the fringes, etc. Experience has shown that $\lambda/200$ can be achieved if the wavefront error does not exceed approximately 20 times this value. The error budget should be adjusted until this criterion is satisfied for the final test and for each stage of calibration.

Secondary Mirror Surface Error ($\lambda/84$)

The mirror surface itself will contribute four times its surface error to the test wave front. The $\lambda/84$ value was chosen as an appropriate value, slightly better than the required $\lambda/80$.

As Table 1 shows, the implied surface is $\lambda/65$. This is disappointing. We have made very high quality test components, constructed an exact geometry setup, gained a factor of four in sensitivity between wavefront and surface and made the mirror better than specification. Yet we can't prove it!

If the sources of error in Table 1 are examined, we note that the most influential error is the secondary itself (as it should be). What happens if we improve the mirror? Figure 6 shows this relationship. The mirror would have to be fabricated to better than $\lambda/120$ to prove it was good to $\lambda/80$.

We might examine the other elements of the error budget in a similar manner. For example, could we reduce the errors contributed by the Hindle Shell? As pointed out earlier, these errors result from components already made about as well as the state of the art allows so not much can be gained there. The other errors in the budget are so small that reducing them would have little effect upon the bottom line number.

The problem originates from the fact that the error of the secondary surface cannot be separated from other errors and uncertainties within the test setup. If this separation could be accomplished, our goal would be realized. This can indeed be accomplished by measuring the test setup. The figure requirement for the mirror can be restated to emphasize this relationship (see Figure 7).

The subscripts are the "error" components of our budget (Table 1). In the next section we show how instrumental errors can be reduced through measurement so the test setup contributions (A) and (B) are eliminated and replaced by a small data reduction contribution. This process of measurement and data subtraction we will define as "calibration".

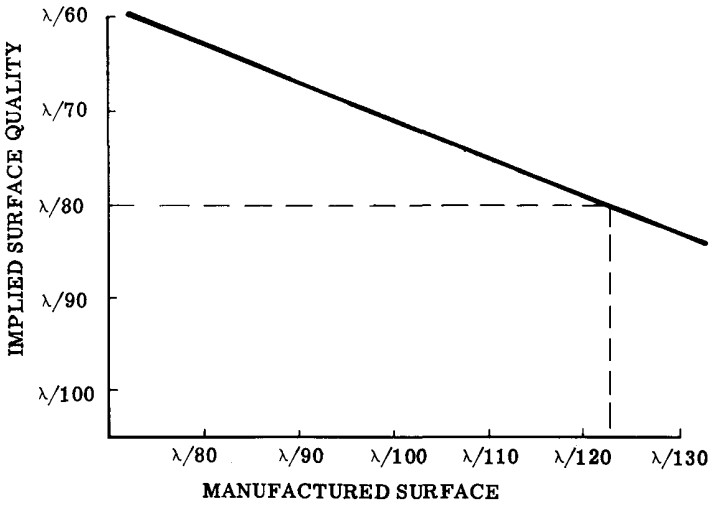

Fig. 6. Results of a better secondary.

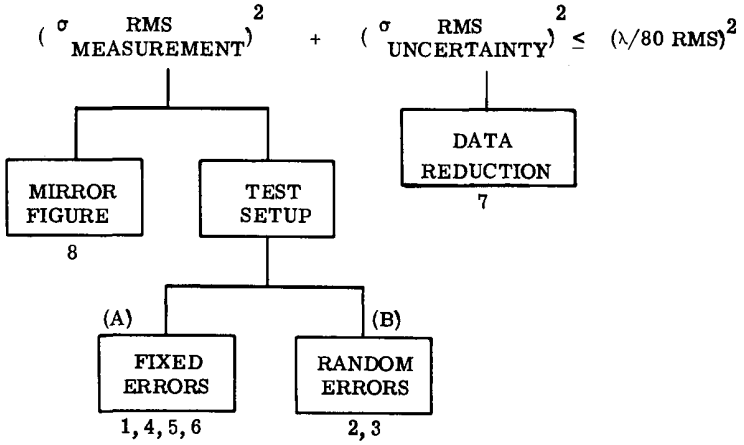

Fig. 7. Measurements – fixed and random errors.

Calibration

The Hindle Shell configuration lends itself to calibration of most of the test errors. In this arrangement the combined effect of the individual contributions is calibrated directly.

Figure 4 and 5 were used previously to illustrate the establishment of the two foci F_1 and F_2. Figure 4 shows the test beam in transmission through the Hindle Shell. The following error sources are included in this beam: design residual, opto-mechanical uncertainties, Hindle Shell transmitted wavefront error, interferometer wavefront error, and the additional error of the calibration sphere. However, the calibration sphere can be tested independently and it can be rotated relative to the shell to separate its errors. Thus, the configuration of Figure 4 can be calibrated to within the limits of data reduction.

Figure 5 shows the reference surface of the Hindle Shell being tested with an interferometer. By rotating the Hindle Shell with respect to the interferometer, the asymmetric errors of the shell can be separated from those of the interferometer. The reference surface of the shell can therefore also be calibrated to within the limits of data reduction.

The remaining errors of Table 1 have to do with the secondary itself, i.e., the surface quality and alignment. Here also we find the ever-present data reduction limit. It is not the intent of this paper to examine data reduction techniques. Some helpful discussion may be found in an article by Parks[3] and in the popular text by Malacara[4].

The calibration sequence has introduced additional equipment and their associated errors. The uncertainties associated with these errors can be calibrated out. Examples of this can be found in recent articles by Slomba[5] and Montagnino[6].

Final Error Budget

The uncertainties included in the original error budget have been substantially reduced to a data reduction limit through calibration. Table 2 summarizes these results. Now we have a test which realistically evaluates the actual surface errors.

Table 2. Hindle Shell Test - Error Sources

Random		Double-Pass rms Contribution
• Transmitted wavefront uncertainty: (after fixed errors are subtracted)		λ/180
– Design Residual – Opto-mechanical uncertainties – Transmitted wavefront error – Interferometer wavefront error	Original Error Sources	
• Hindle Shell reflecting surface uncertainty:		λ/180
• Alignment uncertainty of aspheric secondary:		λ/500
	Subtotal =	λ/123
Fixed		
• Surface quality of aspheric secondary (λ/84):		λ/21
	Calculated total rms residual wavefront =	λ/20.7
	Implied rms surface quality = 1/4 total =	λ/82.8

Summary

It has been shown that by carefully choosing the test configuration, using appropriate data reduction techniques and calibration of the test setup, one can reliably measure the surface figure of a high-quality convex hyperboloid. This was achieved using test components with imperfections of the same order as the surface quality of the aspheric secondary itself.

These methods can be expanded to other conicoids if a test configuration is selected which allows setup calibration independent of the part to be tested. It should be noted that in practice the Hindle Sphere test configuration does not meet this criterion because of scale. Noting that, in general, calibration is limited by the data reduction required for each calibration, it is clear that the number of required calibration steps should be carefully considered and minimized in designing the test setup.

Acknowledgements

We thank R. Casas, F. Foster and A. Offner of the Perkin-Elmer Optical Design Department, and J. Magner of our Metrology Department for their very helpful discussions on this topic.

References

1. Hindle, John H., "A New Test for Cassegrainian and Gregorian Secondary Mirrors," Monthly Notices of the Royal Astronomical Society, March, 1931, reprinted in Amateur Telescope Making, Book One, ed. Albert G. Ingalls (Scientific American Incorporated, 1951). p. 225.

2. Simpson, F. A., Oland, B. H. and Michel, J., "Testing Convex Aspheric Lens Surfaces with a Modified Hindle Arrangement", Opt. Eng.,13, G101 (1974).

3. Parks, R. E., "Removal of Test Optics Errors", SPIE Proceedings, Vol. 153, p. 56.

4. Malacara, D., Optical Shop Testing, Wiley and Sons, 1978.

5. Slomba, A. F., "Application of Lasers to Measure the Optical, Thermal and Mechanical Properties of Materials", SPIE Proceedings, Vol. 92, p. 31.

6. Montagnino, L. A., and Offner, A. "Design and Testing with a Reflective Null System", presented at 21st annual meeting of the American Astronautical Society, August 1975.

Question submitted by Bob Parks (Optical Sciences Center, U of A):
Was the paper addressing the space telescope secondary in particular?

Answer: No. The talk is directed at conicoids in general. The hyperbolic configuration was selected as an example because it is sufficiently complex to illustrate the advantages of the calibration procedure.

Question submitted by Al Parr (Farrand Optical):
Because of the significant effect of the Hindle Shell manufacturing errors, did you make much use of sector or annular masking and rotating to get the statistical advantage of many measurements to minimize the effect of any poor sector or annulus of the Hindle Shell?

Answer: The example was a hypothetical one, but, because of the symmetry of the test, any component of the test may be rotated to identify asymmetric defects. The measurement sequence which was presented will automatically remove such effects since the total measurement and the setup calibration measurements will contain the same contribution and hence can be subtracted on a point-by-point basis.

Question submitted by J. Zimmerman (Honeywell Electro-Optics Center):
How would you handle surface deformations due to the effects of mounting?

Answer: Test component mounting deformations are calibrated out in the test sequence presented.

Question submitted by Al Brunsing (Coulter Electronics):
Does your test measure the local errors on the test hyperboloid due to scattering (scratch and dig) and surface inaccuracies?

Answer: The test as presented is designed to measure surface deformation. The spatial frequency range that is included is determined by the fringe density that the interferometer is capable of handling.

Question submitted by Mark Egdall (ITEK):
Should not the environmental effects (vibration, turbulence, gravity) also be error budgeted and methods to remove them proposed?

Answer: The error budget presented is not intended to be all inclusive, however these random effects are accumulated in the data reduction budget.

Question submitted by Cy Denny (SPAWR):
Is there value in rotating only the tested element to separate it from the system - followed by data reductions of at least 1/4 sections?

Answer: Yes, there is definite advantage to this procedure. The written version of the paper addresses this topic.

Question submitted by B. Brady (Applied Optics Center):
What is the cost tradeoff between conventional Hindle testing and using the Hindle shell?

Answer: The aperture of the Hindle shell is much smaller than the Hindle Sphere for most applications. This implies less cost for manufacturing the shell, a smaller mount, a smaller diameter vacuum chamber, etc. These cost advantages should be compared to the cost of the material for the shell and the working of two optical surfaces.